Pharmacologic inhibition of EPHA2 decreases inflammation and pathological endochondral ossification in osteoarthritis

Authors: Mauricio N. Ferrao Blanco [1], Raphaelle Lesage [2,3], Nicole Kops [1], Niamh Fahy [1, 4, *], Fjodor T. Bekedam [1], Athina Chavli [1], Yvonne M. Bastiaansen-Jenniskens [1], Liesbet Geris [2,3,5], Mark G. Chambers [6], Andrew A. Pitsillides [7], Roberto Narcisi [1], Gerjo J.V.M. van Osch [1,8,9]

Affiliations: [1] Department of Orthopaedics and Sports Medicine, Erasmus MC, University Medical Center Rotterdam, Rotterdam, The Netherlands. [2] Prometheus, Division of Skeletal Tissue Engineering, KU Leuven, Belgium. [3] Biomechanics Section, KU Leuven, Belgium. [4]Department of Oral and Maxillofacial Surgery, Erasmus MC, University Medical Center Rotterdam, Rotterdam, The Netherlands. [*] Current affiliation. Department of Applied Science, Technological University of the Shannon: Midlands Midwest, Limerick, Ireland. [5]GIGA In silico medicine, University of Liège, Belgium. [6] Lilly Research Laboratories, Eli Lilly Pharmaceuticals, Indianapolis, USA. [7] Comparative Biomedical Sciences, Royal Veterinary College, London, United Kingdom. [8] Department of Otorhinolaryngology, Erasmus MC, University Medical Center Rotterdam, Rotterdam, The Netherlands. [9] Department of Biomechanical Engineering, University of Technology Delft, Delft, The Netherlands.

Abstract

Low-grade inflammation and pathological endochondral ossification are processes that underlie the progression of osteoarthritis. In this study, data mining on publicly available transcriptomic datasets revealed EPHA2 to be associated both with inflammation and endochondral ossification in osteoarthritis. EPHA2 was further investigated using a computational model of cellular signaling networks in chondrocytes. *In silico* activation of EPHA2 increased inflammatory mediators and triggered the hypertrophic differentiation of healthy chondrocytes, the phenotypic switch characteristic of endochondral ossification. Inhibition of EPHA2 in cultured chondrocytes isolated from individuals with osteoarthritis reduced inflammation and hypertrophy. Systemic subcutaneous administration of the EPHA2 inhibitor ALW-II-41-27 attenuated joint degeneration in a mouse model, attenuating local inflammation and pathological endochondral ossification. Collectively, we demonstrate that pharmacological inhibition of EPHA2 with ALW-II-41-27 is a promising disease-modifying treatment that paves the route for a novel drug discovery pipeline for osteoarthritis.

Introduction

Osteoarthritis (OA) is the most prevalent and disabling musculoskeletal disease worldwide [1], characterized by progressive joint changes leading to pain and disability [2, 3]. In OA the joint is inflamed, the cartilage lining the joint surface is lost and bony spurs (called osteophytes) are formed at the joint margins. Current pharmacologic treatments are palliative, predominantly pain killers, that do not halt disease progression. Thus, there is an urgent need to discover disease-modifying OA drugs (DMOADs) that can alleviate the development of OA.

Chondrocyte hypertrophy is a chondrocyte phenotype that precedes cartilage calcification and ultimately its replacement by bone. Under physiological conditions, articular chondrocytes are resistant to hypertrophy. During OA, however, the onset of hypertrophic differentiation drives cartilage breakdown [4]. In a similar way, joint margins are established through the growth of an initial cartilage template that undergoes endochondral ossification and is replaced by bone [5]. Inflammation present during OA is characterized by synovitis, encompassing an increase in macrophage activation and the production of inflammatory cytokines such as tumor necrosis factor alfa (TNF-α) [6, 7]. Inflammatory signaling activation is known to trigger cartilage extracellular matrix degradation, and has been proposed to induce chondrocyte hypertrophy [8, 9].

Therefore, we hypothesize that blocking a key target regulating both chondrocyte hypertrophy and inflammation would be an effective therapeutic strategy for OA.

Thus, in this study we aim to identify a druggable target for OA associated with chondrocyte hypertrophy and inflammation, and determine the efficacy of its pharmacologic inhibition combining *in silico*, *in vitro* and *in vivo* models.

Results

EPHA2 is as an inflammation-related gene upregulated in hypertrophic chondrocytes and osteoarthritic cartilage

To identify a novel therapeutic target for OA associated with chondrocyte hypertrophy and inflammation, we performed data mining on two publicly available murine microarray data sets [10, 11]. Differentially expressed genes (DEG) in articular cartilage of mice where OA was induced by destabilization of the medial meniscus (DMM) compared to cartilage of mice that had sham surgery were considered as OA-related genes. By getting the intersection of this set with another set of DEG in the hypertrophic compared to the proliferative zone of the mouse growth plate, we identified 172 genes differently expressed in OA that were also associated with chondrocyte hypertrophy. Nine of these genes overlapped with the gene ontology inflammatory response [12] (Fig. 1A, B). We then analyzed the expression of these 9 genes in a human microarray dataset obtained from OA and healthy articular cartilage [13], and found that 3 genes were also upregulated in human OA cartilage (Fig. 1C). Among these genes, *GJA1* and *PTGS2* had already been studied in the context of OA [14], while *EPHA2,* which encodes the tyrosine kinase receptor EPHA2, has a currently

unknown role in OA. *EphA2* expression was 30-fold upregulated in OA versus sham mouse articular cartilage (adjusted p-value= 2E-02) [11], and 3-fold upregulated in human OA versus healthy cartilage (adjusted p-value= 1E-08) [13]. Moreover, expression of *EphA2* was found to be 19-fold higher in the hypertrophic compared to the proliferative zone of the murine growth plate (adjusted p-value= 1E-07) [10].

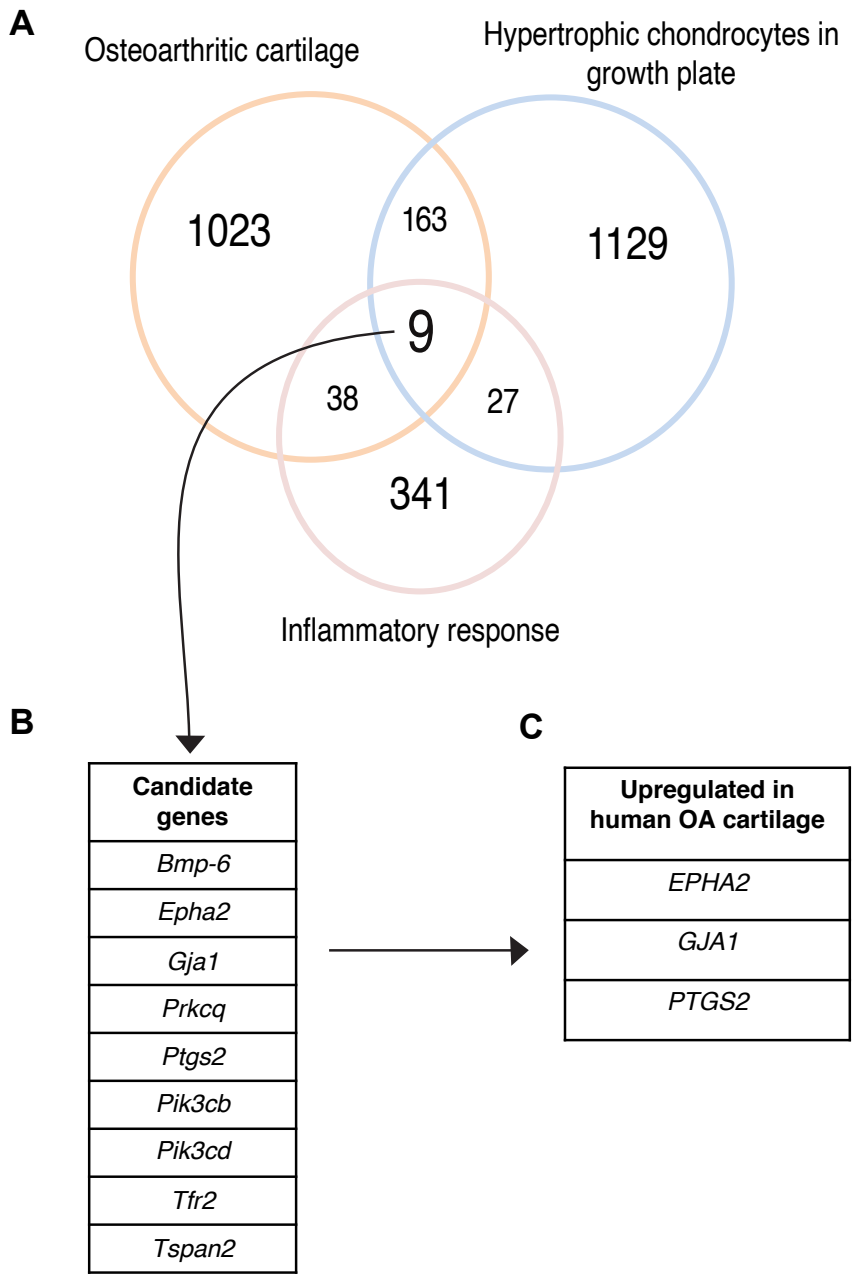

Figure 1. Identification of EPHA2 as a novel target for OA associated with inflammation and chondrocyte hypertrophy. (A) The Venn diagram illustrates the genes related to the inflammatory response, genes that were differentially

regulated in murine osteoarthritic cartilage (DMM vs sham) and genes differentially expressed in the murine growth plate (proliferative vs hypertrophic zone). The number of genes in each dataset [10, 11] is represented, together with those that overlapped. (B) List of 9 targets that overlapped in the three databases. (C) Target genes upregulated in human OA compared with healthy articular cartilage [13]. DEGs with a fold change greater than 3, and an adjusted p value lower than of 0.05, were considered for the analysis

EPHA2 triggers inflammatory markers and induces chondrocyte hypertrophy *in silico*

To evaluate the role of EPHA2 in the regulation of chondrocyte homeostasis, we used a computational model of articular chondrocyte regulatory pathways. This model enables the *in silico* screening of molecular targets in early stages of drug discovery [15]. This mechanistic model combines knowledge-based data of chondrocyte regulatory pathways, which consists of 60 biological components including growth factors, receptors, transcription factors, extracellular matrix proteins and signaling molecules. They form a strongly interconnected network, regulated at the transcriptional and post-translational levels. EPHA2 was integrated into the network considering its previously reported interactions with the following components of the *in silico* model: Wingless and Int-1 (Wnt) [16], Dishevelled (DSH) [17], Nuclear factor kappa B (NFκB) [18], Protein kinase B (Akt) [19], extracellular signal-regulated kinase (Erk) 1/2 [20],

phosphatidylinositol 3-kinase (Pi3k) [21, 22] and Rat sarcoma virus (Ras) [23] (Fig. 2A). Two mathematically stable states emerged from this model, that akin to previous versions of the model equated to two possible cellular states (i.e. chondrocyte phenotypes) [15]. Among the main characteristics of hypertrophic chondrocytes there is the upregulation of Matrix Metallopeptidase (*MMP13*), type 10 Collagen (*COL10A1*) and Runt-related transcription factor 2 (*RUNX2*) whereas healthy chondrocytes are characterized by the expression of type II collagen (*COL2A1*), Aggrecan (*ACAN*) and SRY-box transcription factor (*SOX9*) [24]. Based on the characteristic expression of these markers, we identified one stable state as 'healthy' and the other as 'hypertrophic' chondrocyte (Fig. 2A and supplementary figure 1), similar to what was observed in previous versions of the model [15]. The biological entities present in the model that relate to inflammation –specifically inflammatory cytokines, transforming growth factor-β-activated kinase (TAK) 1 and NFκB – were only active in the hypertrophic phenotype (see predicted hypertrophic activity profile in Fig. 2A), which aligns with the proposed close relationship between inflammation and hypertrophy. The variable representing EPHA2 was active in the hypertrophic while inactive in the healthy state (Fig 2A and supplementary figure 1). *In silico* experiments were performed to test the capacity of EPHA2 to induce inflammation and hypertrophy (Fig. 2B). Activation of EPHA2 triggered the transition of healthy articular chondrocytes towards the inflammatory hypertrophic state to a greater extent than the activation of the inflammatory cytokines and their receptors (9% and 5% for

the conditions ‘EPHA2+’ and ‘Inflammation+’, respectively; Fig. 2C). As a result, both conditions initiated a decrease of anabolic markers (COL II, Aggrecan: blue vs orange and yellow bars; Fig. 2D) and an increase of hypertrophic and inflammatory markers (Fig. 2D, 2E). Activation of both EPHA2 and the inflammatory cytokines with their receptors had a robust synergistic effect, reaching 100% transition of healthy chondrocytes towards the inflammatory hypertrophic state (‘Inflammation+ EphA2+’; Fig. 2C). Interestingly, this switching of cellular state was abolished when inhibiting EPHA2 (Inflammation+ EPHA2-; Fig. 2C), with a strong reduction of the activity of hypertrophic and inflammatory entities (green vs violet and yellow bars; Fig. 2 D & E). These *in silico* results support the hypertrophic and inflammatory role of EPHA2 in chondrocytes.

A

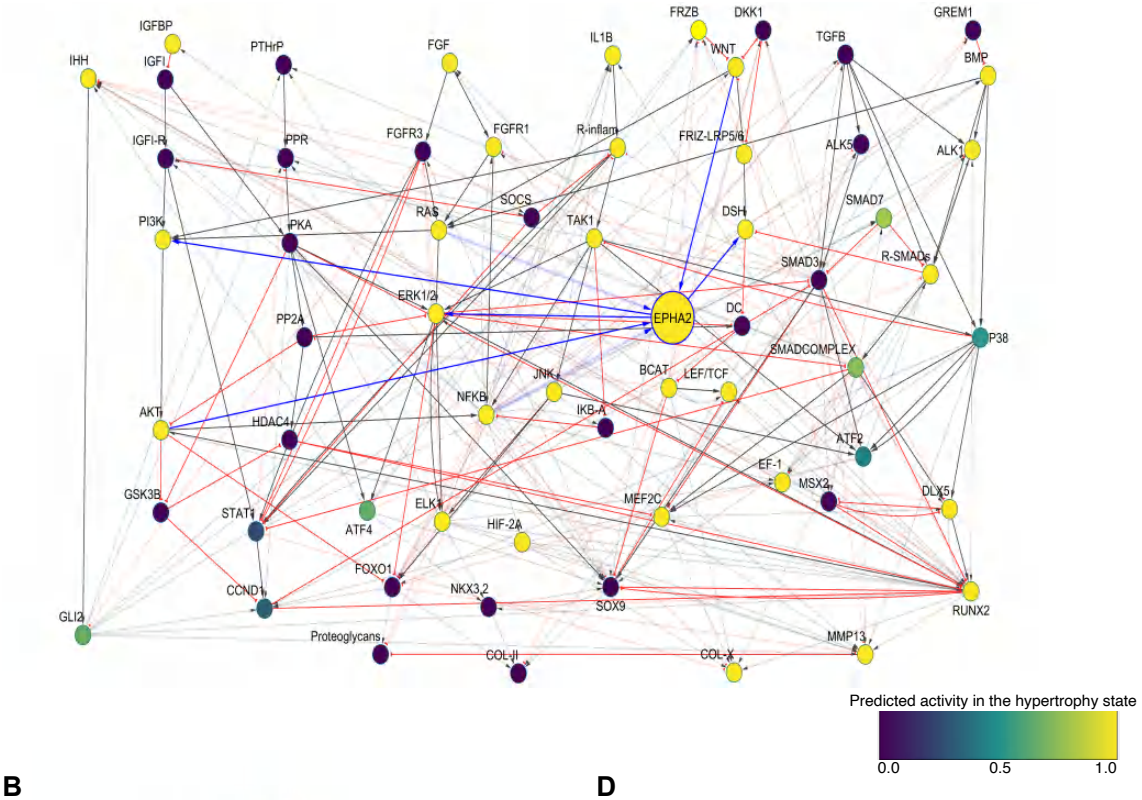
IGFBP
IGFI
IHH
PTHrP
FGF
IL1B
FRZB
DKK1
WNT
TGFB
GREM1
BMP
IGFI-R
PPR
FGFR3
FGFR1
R-inflam
FRIZ-LRP5/6
ALK5
ALK1
PI3K
PKA
RAS
SOCS
TAK1
DSH
SMAD7
SMAD3
R-SMADs
ERK1/2
EPHA2
DC
PP2A
P38
SMADCOMPLEX
JNK
BCAT
LEF/TCF
NFKB
IKB-A
AKT
HDAC4
ATF2
EF-1
MSX2
DLX5
GSK3B
STAT1
ATF4
ELK
MEF2C
HIF-2A
FOXO1
CCND1
NKX3.2
SOX9
RUNX2
GLI2
Proteoglycans
COL-II
COL-X
MMP13
Predicted activity in the hypertrophy state
0.0
0.5
1.0

B

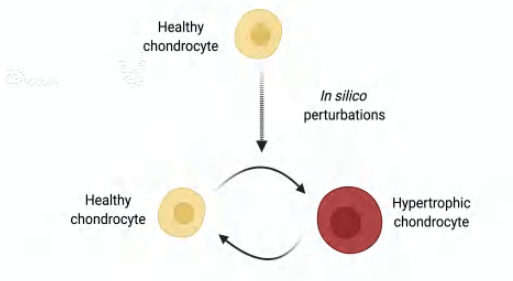
Healthy chondrocyte
In silico perturbations
Healthy chondrocyte
Hypertrophic chondrocyte

D

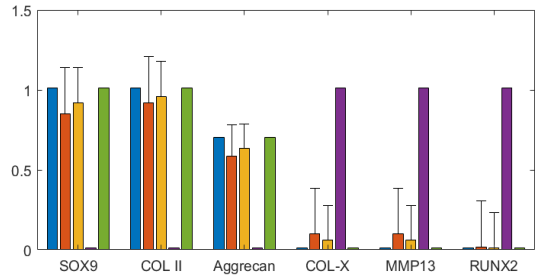
1.5
1
0.5
0
SOX9
COL II
Aggrecan
COL-X
MMP13
RUNX2

C

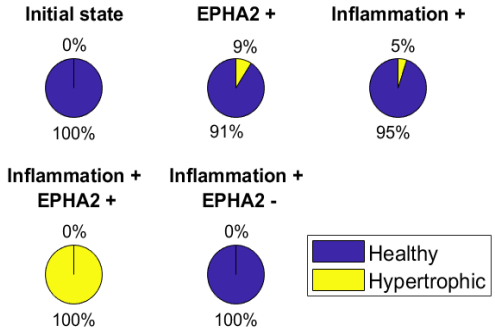
Initial state
0%
100%
EPHA2 +
9%
91%
Inflammation +
5%
95%
Inflammation + EPHA2 +
0%
100%
Inflammation + EPHA2 -
0%
100%
Healthy
Hypertrophic

E

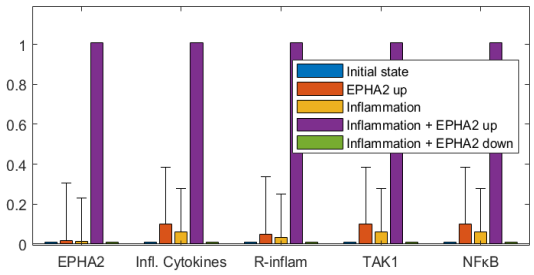
1
0.8
0.6
0.4
0.2
0
Initial state
EPHA2 up
Inflammation
Inflammation + EPHA2 up
Inflammation + EPHA2 down
EPHA2
Infl. Cytokines
R-inflam
TAK1
NFκB

Figure 2. EPHA2 activation induces chondrocyte hypertrophy and inflammation *in silico* (A) Integration of EPHA2 in the regulatory network of articular chondrocytes. Solid lines denote protein interaction while modulation at the gene level is in dotted lines. Activating interactions are in grey with delta arrows and inhibitory interactions are in red with a half circle. Connections with EPHA2 are denoted in blue. All components of the model are represented with a variable that is named with capital letters. The variable represents neither the protein activation level nor the gene expression but a product of both (global activity). The color of the nodes in the network denotes the global activity of the variables in the hypertrophic state, with dark blue being 0 and yellow being 1. (B) Scheme of the *in silico* experiment. (C) Activation of EPHA2 in the healthy state promotes the transition to a hypertrophic phenotype. Forced activation (+) or inhibition (-) of the entities from the initial healthy state is shown. Inflammation represents the activation of the variables related to inflammatory cytokines and their receptors, as input in the model. Pie charts represent the predicted percentage of perturbations leading to a transition to the hypertrophic phenotype or remaining in the healthy phenotype. (D) Average activity of the chondrogenic markers, being type II collagen, Aggrecan and SRY-box transcription factor (SOX9), and of hypertrophic markers, being Runt-related transcription factor 2 (RUNX2), Matrix Metallopeptidase (MMP13) and type 10 Collagen. (E) Average activity of EPHA2 and variables associated with inflammation. The bars represent the mean of the results of a hundred *in silico*

experiments (+ standard deviations, +SD). There is no SD for the initial state (blue condition) as it denotes the starting point before the *in silico* perturbation is applied. Figure created with Cytoscape, MATLAB and Biorender.com

ALW-II-41-27 reduces human OA-derived chondrocyte inflammation

To explore whether pharmacological inhibition of EPHA2 could be used to reduce inflammation in OA, we used the tyrosine kinase inhibitor ALW-II-41-27 *in vitro* on TNF-α-treated human chondrocytes from OA donors (Fig. 3A). This small molecule is a type II kinase inhibitor with high selectivity for EphA2 [25, 26]. Addition of ALW-II-41-27 effectively inhibited the TNF-α-induced inflammatory activity as shown by a 3-fold reduction in the secretion of nitric oxide metabolites (Fig. 3B). Likewise, administration of ALW-II-41-27 attenuated the TNF-α-induced expression of the inflammatory cytokine interleukin (IL)-6 at the gene (4-fold, Figure 2C) and protein level (5-fold, Figure 2D), known to be a downstream target gene of TNF-α via NFκB [27]. Furthermore, ALW-II-41-27 treatment counteracted the TNF-α-induced upregulation of the cartilage matrix degrading enzymes *MMP1* (6-fold, Figure 3E) and *MMP13* (4-fold, Figure 3F). These results demonstrate the anti-inflammatory capacity of ALW-II-41-27 in TNF-α-stimulated OA chondrocytes.

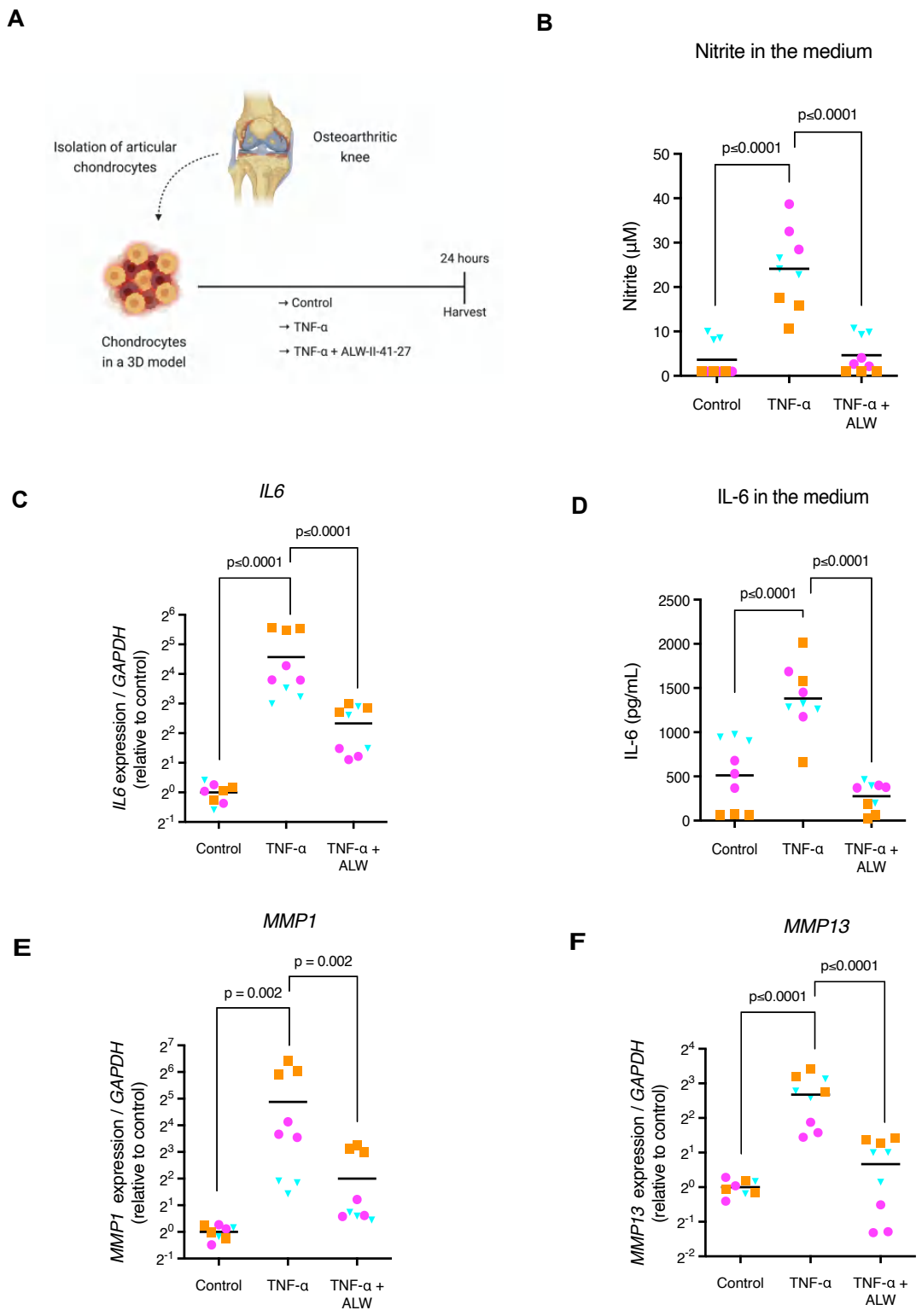

Figure 3. ALW-II-41-27 decreases TNF-*α* induced catabolism and inflammation in human chondrocytes. (A) Experimental set-up to evaluate the anti-inflammatory capacity of ALW-II-41-27 (10 μM) in human OA

chondrocytes cultured with 10 ng/mL TNF-α. (B) Evaluation of nitrite in the medium as a marker for inflammatory activity as determined by Griess reagent. (C, E-F) Gene expression of *IL6*, *MMP1* and *MMP13* determined by qPCR. The average of control, per donor, is set to 1. (D) IL-6 in the medium determined by ELISA. Experiments were performed in triplicate, with cells from three donors. Donors are represented with different colors and symbols: violet circles (donor 1), blue triangles (donor 2) and orange squares (donor 3). The horizontal line in the graphs represents the mean. Data were analyzed with the linear mixed model with Bonferroni's multiple comparisons test. Figure created with Biorender.com

ALW-II-41-27 decreases chondrocyte hypertrophy

We then proceeded to evaluate whether pharmacological inhibition of EPHA2 with ALW-II-41-27 inhibits hypertrophy in human OA-derived articular chondrocytes (Fig. 4A). ALW-II-41-27 decreased *COL10A1* expression 2-fold (Fig. 4B), suggesting a reduction in hypertrophy. Since chondrocyte hypertrophy is a key process that hinders stable hyaline cartilage tissue engineering [28], we further investigated the effect of ALW-II-41-27 on cartilage tissue engineered constructs from mesenchymal stem cells (MSCs), well-known to become hypertrophic and prone to ossify when implanted *in vivo* [29-32] (Fig. 4C). Gene expression analysis revealed that the addition of ALW-II-41-27 attenuated the hypertrophic markers *COL10A1* and *ALPL* by a fold change of 2 and 3, respectively (Fig. 4D & E). Accordingly, when treated with ALW-II-41-27 the

cells deposited less type X Collagen (Fig. 4F and supplementary figure 2). Interestingly, neither glycosaminoglycan nor type II Collagen deposition was reduced (Fig. 4F), suggesting that ALW-II-41-27 was mainly targeting hypertrophy.

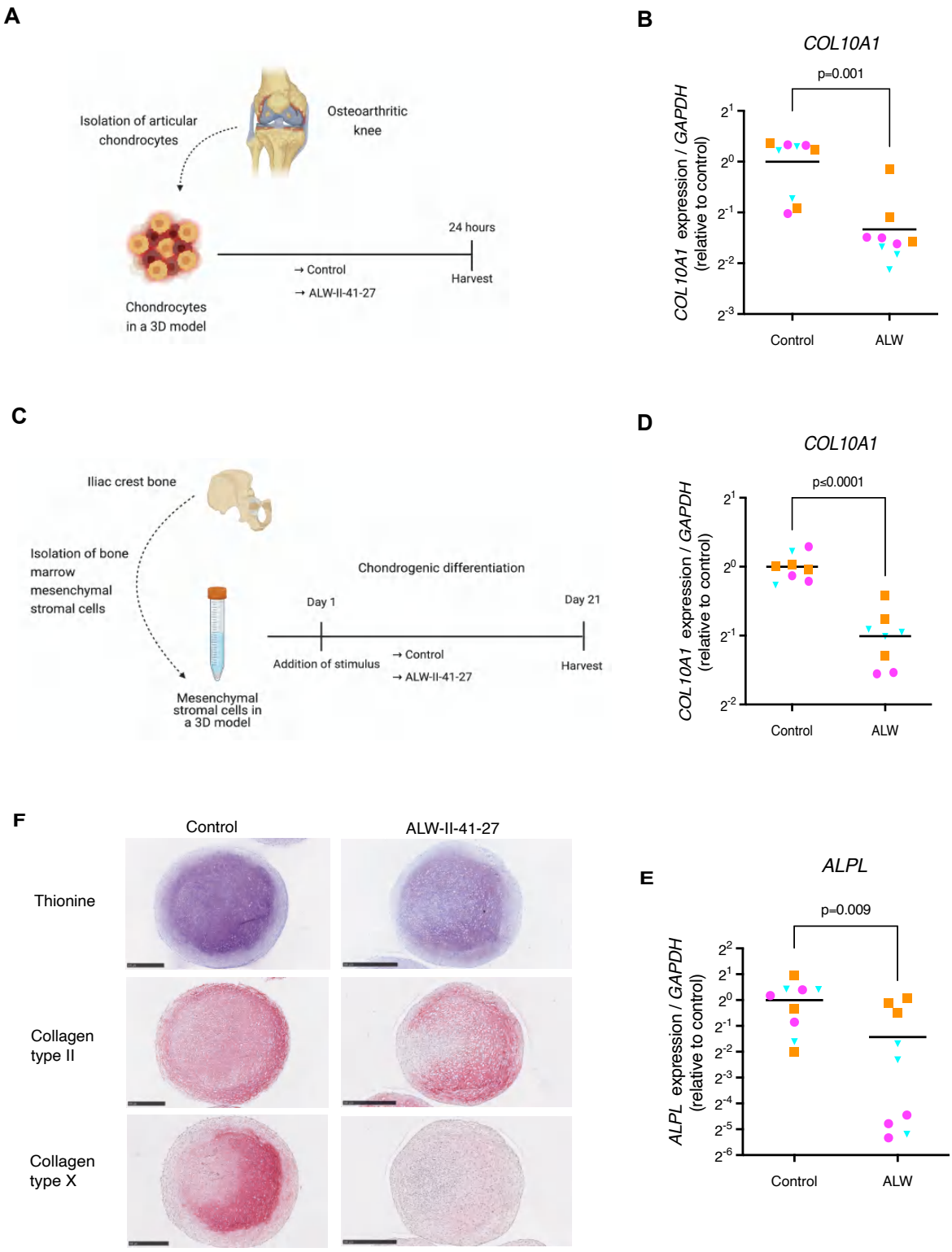

Figure 4. ALW-II-41-27 decreases chondrocyte hypertrophy. (A) Experimental set-up to evaluate the capacity of ALW-II-41-27 (10 µM) to modulate hypertrophy in human OA chondrocytes. (B) Gene expression of the

hypertrophic marker *COL10A1* in cultured OA chondrocytes determined by qPCR. (C) Experimental set-up to evaluate how ALW-II-41-27 (100 nM) affects hypertrophy in tissue engineered cartilage from MSCs. (D, E) Gene expression of *COL10A1* and *ALPL* in MSC-generated cartilage determined by qPCR. (F) Histological analysis of tissue engineered cartilage derived from MSCs; Thionine staining showing glycosaminoglycans (violet), and immunohistochemistry of type II and type X collagen (red/pink). Experiments were performed with 3 replicates, for each of the three donors. Donors are represented with different colors and symbols: violet circles (donor 1), blue triangles (donor 2) and orange squares (donor 3). For gene expression analysis, the average of control replicates is set to 1 per donor. The horizontal line in the graphs represents the mean. For statistical analysis, the linear mixed model with Bonferroni's multiple comparisons test was performed. Figure created with Biorender.com

ALW-II-41-27 treatment reduces joint inflammation and pathological endochondral ossification *in vivo*

EPHA2 inhibition reduced hypertrophy and inflammation *in silico* and its pharmacological inhibition with ALW-II-41-27 in cell culture *in vitro* confirmed these results. Therefore, we proceeded to evaluate whether ALW-II-41-27 could be an effective OA therapy *in vivo* using a mouse model of joint pain and degeneration following intra-articular injection of monoiodoacetate (MIA) [33]. ALW-II-41-27 was subcutaneously administered with a controlled delivery

system (Fig. 5A). Total body weight was not affected by the administration of ALW-II-41-27 over the 14 days of the study, suggesting no significant effects of the treatment on the general health state of the animals (supplementary figure 3). Treatment with ALW-II-41-27 reduced the synovial membrane thickness (Fig. 5B, C & D) as well as synovitis (Fig. 5E) as compared to vehicle-treated mice. Synovitis is governed by macrophages, the crucial regulators of OA progression and primary mediators of the inflammatory response [34, 35]. Macrophages were observed only in the synovial lining of vehicle-treated mice, indicating that ALW-II-41-27 effectively attenuated joint inflammation (Fig. 5F). Monocytes migrate from the circulation into tissues under inflammatory conditions and differentiate into macrophages [36, 37]. To investigate whether the observed decrease in local joint inflammation following ALW-II-41-27 administration was associated with a systemic effect on immune cells, we also examined potential effects on peripheral blood monocytes. At day 2 and 12, the levels of monocytes in blood were not altered compared to vehicle-treated mice (Fig. 5G), suggesting that the drug selectively decreased local joint inflammation.

Since joint pain is a major symptom in OA often associated with inflammation [38, 39], we investigated this parameter by evaluating distribution of weight between the limbs of the mice. However, no significant difference was detected between ALW-II-41-27-treated and vehicle-treated mice, suggesting no effect was apparent on pain (supplementary Figure 4).

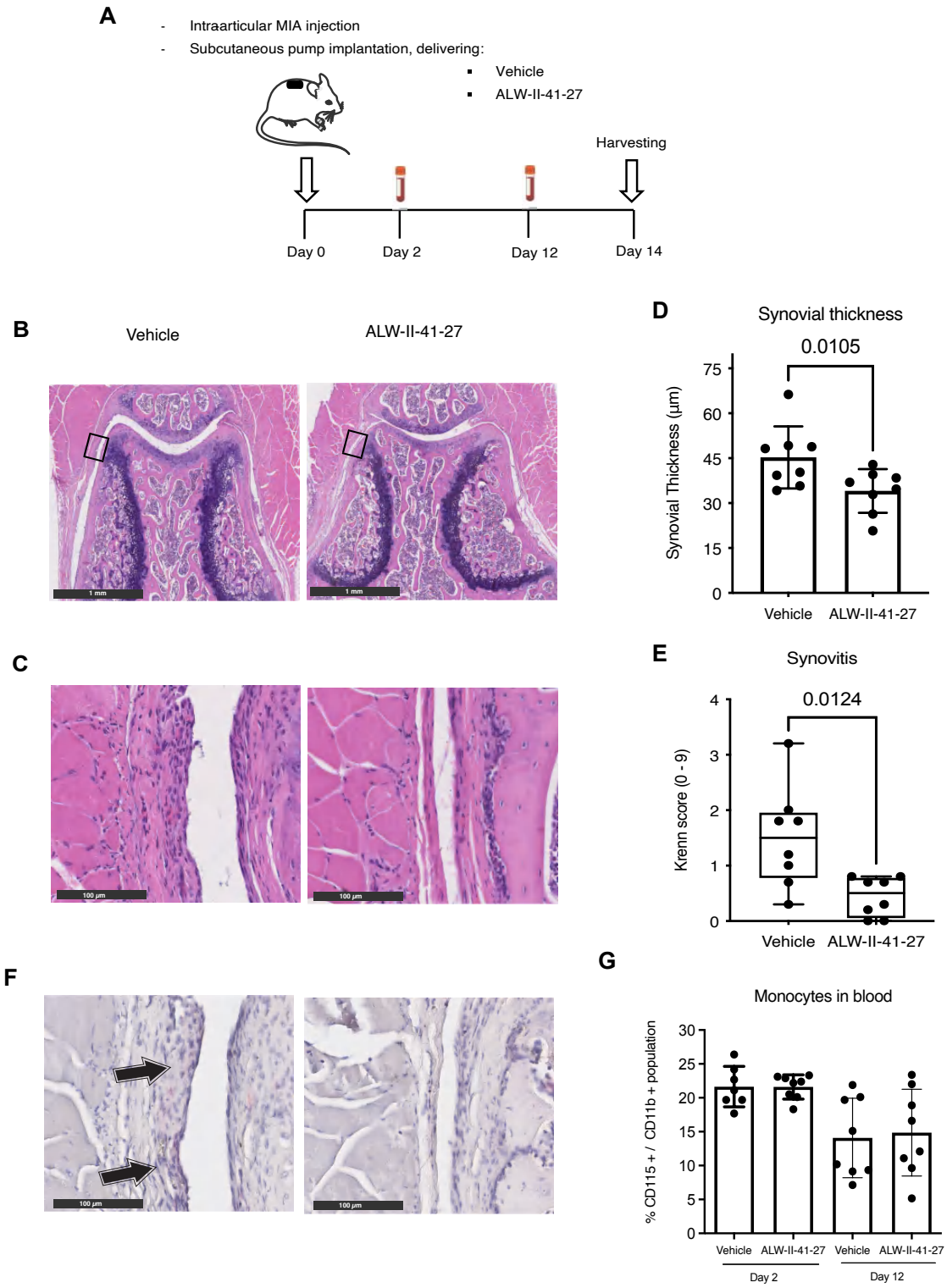

Figure 5. ALW-II-41-27 treatment attenuates joint inflammation. (A) Experimental set-up of the *in vivo* experiment. Intra-articular injection of monoiodoacetate (MIA, 60 µg in 6 µl of saline) was applied to the right knee of

mice for each experimental group (N=8) to induce OA. An osmotic pump was implanted on the back of the mice, slightly posterior to the scapulae, which continuously delivered vehicle or ALW-II-41-27 in a dose of 6.6 μg/ hour. At day 2 and 12 peripheral blood was harvested. At day 14 mice were euthanized to assess the effects of ALW-II-41-27 on the degenerated joint. (B) Hematoxylin and Eosin staining of knees (patellofemoral region) from vehicle-treated and ALW-II-41-27-treated mice. Black square indicates the region of magnification for the image below (C) showing the synovial lining where synovial thickness and Krenn score were determined. (D) Synovial thickness is represented by the mean ± SD. (E) Krenn score illustrated with box-and-whiskers plots, with line indicating the median and error bars spanning maximum to minimum values. (F) Immunohistochemistry of F4/80 (pink) showing macrophages in the synovial lining. Arrows indicate positive staining. (G) Percentage of monocytes present in the peripheral blood of mice at day 2 and 12, respect to the myeloid cell population. In all graphs, each dot represents data of an individual mouse (N=8). For statistical analysis, the linear mixed model with Bonferroni's multiple comparisons test was performed. Figure created with Biorender.com

Since cartilage damage and osteophyte formation are prominent pathophysiological features of OA, we next interrogated whether ALW-II-41-27 modulates cartilage damage and osteophytosis in the joint. Cartilage degeneration was observed by loss of proteoglycans and was exhibited in all mice regardless

of the treatment with ALW-II-41-27 (Fig. 6 A&B), suggesting that ALW-II-41-27 was not able to rescue matrix degeneration *in vivo*. Histological assessment of the knee joints showed that osteophytes, particularly present at the lateral side of the patella (Fig. 6C), were significantly smaller in ALW-II-41-27-treated mice (Fig. 6D). Accordingly, type X collagen deposition was decreased in the knees of ALW-II-41-27-treated mice (Fig. 6E). These results indicate that subcutaneous delivery of ALW-II-41-27 effectively targets endochondral ossification in the injured joint.

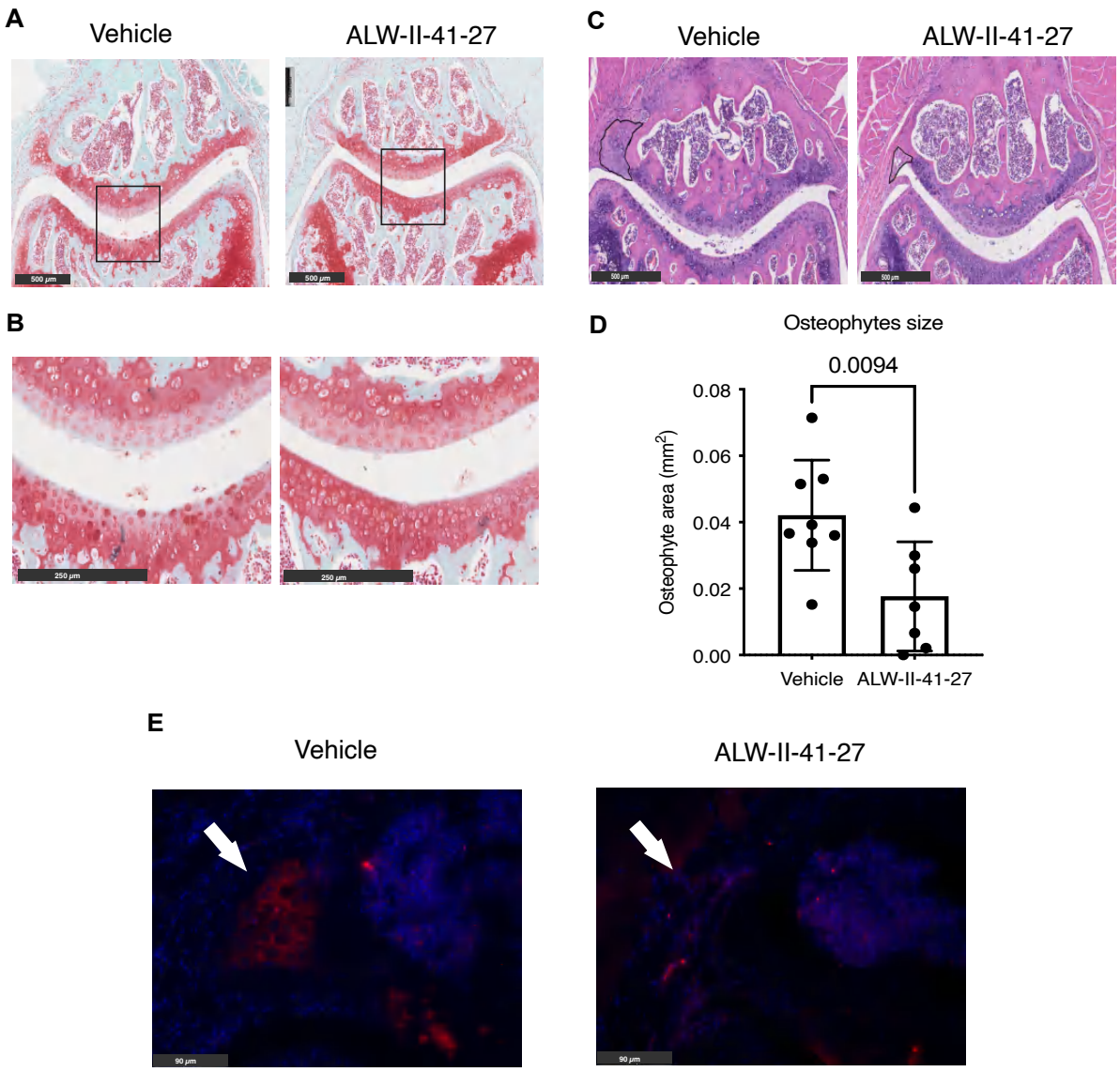

Figure 6. ALW-II-41-27 treatment attenuates pathological endochondral ossification (A) Safranin-O / Fast Green staining of vehicle-treated and ALW-II-41-27-treated mice knees with magnification of the patellofemoral region. Black

square indicates the region of magnification for the image below (B) showing the central part of the patellofemoral articular cartilage. (C) Hematoxylin and Eosin stain of vehicle-treated and ALW-II-41-27-treated mice knees with magnification of the patellofemoral region. Osteophyte's diameter is indicated with a black line in the lateral side of the patella. (D) Osteophyte area adjacent to the lateral side of the patella is represented by the mean ± SD. Each dot represents data of an individual mouse (n=8). For statistical analysis, the linear mixed model with Bonferroni's multiple comparisons test was performed (E) Immunofluorescence of type X collagen (red) and DAPI (blue) in the lateral side of the patellofemoral region. Arrow indicates an osteophyte in the lateral side of the patella.

A

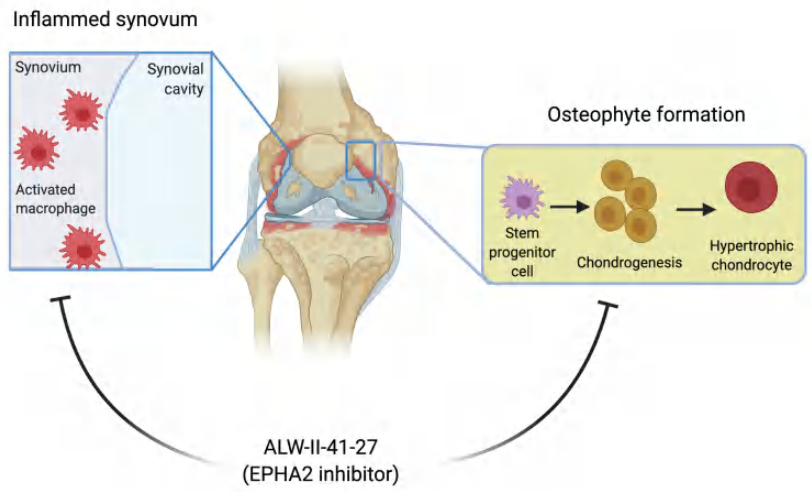

B

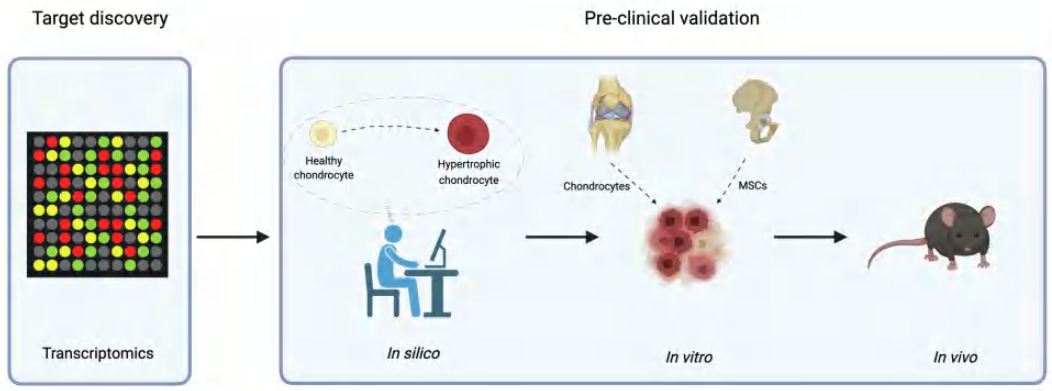

Figure 7. Graphical representation of main findings and experimental approach. (A) ALW-II-41-27 attenuates synovitis and osteophyte formation. (B) Drug discovery pipeline combining transcriptomic datasets, *in silico*, *in vitro* and *in vivo* models. Figure created with Biorender.com

Discussion

There is an urgent unmet need for effective therapies for OA patients. Here, we show that EPHA2 is a promising drug target for OA and we report the small molecule ALW-II-41-27 as a disease-modifying OA drug (DMOAD), specifically targeting inflammation and pathological endochondral ossification (Fig. 7A). To find targets associated with inflammation and chondrocyte hypertrophy we have used a particular sequence of studies that involved *in silico*, *in vitro* and *in vivo* analyses (Fig. 7B). For the i*n silico* analyses we leveraged previously published large gene expression dataset depositories and narrowed them down to one target of interest. The role of the identified target on inflammation and chondrocyte hypertrophy was further investigated through *in silico* experiments using a computational model of cellular signaling networks controlling chondrocyte phenotypes. These *in silico* studies served as the starting point for a series of *in vitro* experiments using different cell models, which were followed by an *in vivo* study. We demonstrate the effectiveness of this experimental approach to identify a new target for specific biological processes in osteoarthritis.

Whereas others have found EPHA2 as a main regulator in diseases such as cancer [40-43] and irritable bowel disease [44], this is the first study, to our knowledge, that highlights the influence of EPHA2 in OA. Other tyrosine kinases, such as fibroblast growth factor receptor (FGFR) 1, Fyn and vascular endothelial growth factor receptor (VEGFR), have been indicated to promote chondrocyte

hypertrophy [45-48]. Here we show that the tyrosine kinase EPHA2 is not only involved in hypertrophy but also in inflammation, making it an attractive target to attenuate pathological drivers in OA.

The mechanism by which EPHA2 modulates chondrocyte hypertrophy and inflammation is not completely decrypted in our study. However, an insight of the signaling pathways is appreciated in the computational chondrocyte model. EPHA2 controls signaling pathways that are key regulators of chondrocyte hypertrophy and inflammation, namely WNT [49], RAS [50], and the PI3K-AKT axis [51]. The regulatory interactions, based on studies performed in other cell types [16-23], were input in the model and this led to the predictions suggesting the pro-hypertrophic and inflammatory role of EPHA2 in chondrocytes. Given that those predictions were further confirmed *in vitro* and *in vivo*, it supports the possible role of the aforementioned mechanistic interactions. Nevertheless, EPHA2 being still largely understudied in cartilage, it is likely that regulatory interactions with other entities of the chondrocyte regulatory network have been overlooked and should be investigated.

In this pre-clinical study, we identified a promising compound, ALW-II-41-27, which showed potential as a DMOAD since it attenuated inflammation and pathological endochondral ossification *in vitro* and *in vivo*. To date, a wide variety of DMOADs targeting chondrocyte hypertrophy have been tested in experimental studies *in vitro* and *in vivo* [52]. Pterosin B, an inhibitor of salt-inducible kinase (Sik) 3, modified OA by preventing chondrocyte hypertrophy

[53]. In a similar manner, Paroxetine, a G protein-coupled receptor kinase (GRK) 2 inhibitor, prevented cartilage degeneration targeting hypertrophy [54]. It is unclear, however, whether those agents have been subjected to further research. Regulatory agencies, such as the Food and Drug Administration (FDA) or the European Medicines Agency (EMA), have not yet approved any existing disease-modifying pharmacological intervention for OA [55]. Considering the pre-clinical data of ALW-II-41-27 to modulate OA pathogenesis and its extensive pharmacological analysis in other diseases [40-44], it is expected that clinical trials with this drug have a lower-risk with higher chance of success.

Next to cartilage hypertrophy, inflammation of the synovium is an important component of OA pathology [56]. Our data show that ALW-II-41-27 also exerts anti-inflammatory effects, which is in agreement with the previously reported anti-inflammatory effects of this molecule in colonic cells *in vitro* and in a model of irritable bowel syndrome *in vivo* [44]. EPHA2 is not only expressed in chondrocytes but also in other cells present in the synovium, such as fibroblasts [57], monocytes [58] and macrophages [59]. Therefore, the underlying anti-inflammatory mechanism observed in mice might also be associated with the action of ALW-II-41-27 on these cells.

Our study has some limitations. In this study we initiated treatment at the same time we induced OA, due to the progressive nature of the disease and the subsequent challenge faced by a DMOAD where extensive structural changes in the joint in end-stage OA might be impossible to reverse. Therefore, the

pharmacological benefits of ALW-II-41-27 to attenuate inflammation and osteophytosis may be best achieved if applied in earlier stages of the disease. Our study failed to show that *in vivo* ALW-II-41-27 administration can prevent either the cartilage loss or pain produced in the MIA mouse model. Additional investigation in other experimental animal models may reveal whether ALW-II-41-27 specifically targets hypertrophy and inflammation, or whether its effect extend to preventing cartilage degeneration and alleviate pain. Moreover, investigation of the possible effect of ALW-II-41-27 on post-traumatic OA or other non-chemically induced forms of OA is needed.

In this study we have applied systemic delivery of the drug *in vivo*. This would be suitable to treat or prevent osteoarthritis development in multiple joints, so called polyarticular OA [60, 61]. Aiming for the clinical translation of the treatment, future studies should evaluate the efficacy of oral administration of ALW-II-41-27 to treat polyarticular OA. Toxicological assessment in mice have been reported for this small molecule, showing no significant histopathologic effects in the heart, liver, or kidney [41]. Therefore, ALW-II-41-27 possess promising characteristics to be translated to OA clinical trials. Of note, common adverse effects of clinically used tyrosine kinase inhibitors are diarrhea and anemia [62, 63], that might be attenuated by dose-escalation. For patients with OA in a single joint, local delivery of ALW-II-41-27 might offer advantages in maximizing the dose to the affected tissues while minimizing systemic side effects, as reported for the CDC-like kinase 2 (CLK2) and dual-specificity

tyrosine phosphorylation-regulated kinase 1A (DYRK1A) inhibitor Lorecivivint, currently in clinical trials for OA [64].

In conclusion, we provide evidence that EPHA2 plays a pathogenic role in OA. Inhibition of EPHA2 with ALW-II-41-27 was effective in halting inflammation and pathological endochondral ossification in *in silico* models, *in vitro* models with human cells and a mouse model, which warrants further research on this candidate disease-modifying OA drug.

Materials and Methods

Evaluation of ALW-II-41-27 in OA chondrocytes

In vitro target validation was performed using chondrocytes isolated from human articular cartilage from OA donors (2 females, one male, age 61, 64 and 69 years). The cartilage was obtained with implicit consent as waste material from patients undergoing total knee replacement surgery. This protocol was approved by the medical ethical committee of the Erasmus MC, University Medical Center, Rotterdam, protocol number MEC-2004-322. Cartilage chips were subjected to protease (2 mg/ml, Sigma Aldrich) in saline for 2 hours followed by overnight digestion with 1.5 mg/ml collagenase B (Roche Diagnostics, Switzerland) in Dulbecco's Modified Eagle's Medium (DMEM) high glucose supplemented with 10% fetal bovine serum. Single cell suspension was obtained by filtrating the cellular solution through a 100 μm filter. The isolated chondrocytes were

expanded in monolayer at a seeding density of 7,500 cells/cm^2 in DMEM high glucose supplemented with 10% fetal bovine serum, 50 μg/ml gentamicin and 1.5 μg/ml fungizone (Gibco, Grand Island, NY, USA). Upon attaining approximately 80% confluency, cells were trypsinized and reseeded at 7,500 cells/cm^2. Cells were used for experiments after three passages. To re-differentiate the expanded articular chondrocytes, a 3D alginate bead culture model was used [65, 66]. Alginate beads were prepared by mixing passage three chondrocytes and re-suspended them in 1.2% (w/v) low viscosity alginate (Kelton LV alginate, Kelko Co, San Diego, CA, USA) in 0.9% NaCl (Sigma Aldrich) at a concentration of 4×10^6 cells/mL. Beads were made by dripping the cell-alginate suspension in 105 mM $CaCl_2$ (Sigma Aldrich) through a 22-gauge needle. Beads were washed with 0.9% NaCl and DMEM low glucose. Beads with a size that deviated from the average after a visual inspection were not included in the experiment. Re-differentiation of chondrocytes was performed in a 24-well plate (BD Falcon) for two weeks in 100 μL/bead DMEM low glucose supplemented with 1% v/v Insulin-Transferrin-Selenium (ITS™ + Premix, Corning, Bedford, MA, USA), 10 ng/ml transforming growth factor beta-1 (TGF-β-1, recombinant human, R&D systems) 25 μg/mL l-ascorbic acid 2-phosphate (Sigma Aldrich), 50 μg/ml gentamicin, and 1.5 μg/mL fungizone (both Gibco). After two weeks, TGF-β-1 was no longer added to the medium and cells were cultured with 10 μM of ALW-II-41-27 (MedChemExpress, Ann Arbor, MI, USA), vehicle (DMSO) and/or with the pro-inflammatory cytokine TNF-α 10 ng/mL for 24 hours. Preliminary

experiments were performed using two doses of ALW-II-41-27, 1 and 10 μM, being 10 μM more effective. Medium and alginate beads were harvested for further analyses.

Animal model

All animal experimentation procedures were conducted with approval by the Animal Ethical Committee of Erasmus University Medical Center (License number AVD101002015114, protocol number 16-691-06). 12-week-old male C57BL/6 mice (C57BL/6J0laHsd, 27.01 g ± 2.05 g; Envigo, Cambridgeshire, UK), were housed in groups of 8 in individually ventilated cages and maintained on a 12 h light/dark cycle with ad libitum access to standard diet and water at the Experimental Animal Facility of the Erasmus MC. Mice were randomly divided into two experimental groups (N=8 per group): Control and ALW-II-41-27-treated mice. For all procedures, mice were anesthetized using 3% isoflurane/0.8 L O_2/min (Pharmachemie BV, Haarlem, the Netherlands). OA was induced unilaterally by intra-articular injections of 60 μg Monoiodoacetate (MIA) (Sigma-Aldrich, St. Louis, USA) in 6 μl of saline (0.9% NaCl; Sigma-Aldrich) at day 0. Injections were performed after a 3-4 mm dermal incision was made to the right knee at the height of the patellar tendon. All intra-articular injections were administered using a 50 μl syringe (Hamilton, Bonaduz, Switzerland) and 30G needle (BD Medical, New Jersey, USA). ALW-II-41-27 was delivered using

Alzet micro-osmotic pumps (Durect Corporation, CA, USA) model 1004, delivery rates of 0.11 μL/ hour, that were implanted subcutaneously on the back of the mice, slightly posterior to the scapulae, immediately after the intra-articular injections. Osmotic pumps were filled with dimethyl sulfoxide: polyethylenglicol alone (55:45 ratio, vehicle-treated group, N=8 mice) or containing 6 mg of ALW-II-41-27 dissolved in vehicle (treated group, N=8 mice) which leads to a dose of 6.6 μg/ hour. A third group of N=8 mice received the implantation of osmotic pumps delivering a dose of 1.7 μg/ hour of ALW-II-41-27. In the figures 5 and 6 we report the 6.6 μg/ hour dose of ALW-II-41-27. Synovial thickness, Krenn score and osteophyte size for all groups can be found in supplementary figure 6. Mice were euthanized in agreement with the Directive 2010/63/EU by cervical dislocation under isoflurane anesthesia 14 days following MIA injection. After which knees were fixed in 4 % formalin (v/v) for 1 week, decalcified in 10 % EDTA for 2 weeks and embedded in paraffin. Coronal sections of 6 μm were cut for analyses.

Data and statistical analyses

Statistical evaluation was performed using GraphPad Prism 9.0 and IBM SPSS 24 (IBM). Each *in vitro* experiment included at least 3 biological replicates and was repeated with cells derived from 3 donors. The *in vivo* study was designed to generate groups of equal size, used randomization and blinded analyses. The

declared group size is the number of independent values that were used for statistical analysis. Sample size for the *in vivo* study was calculated considering the weight distribution over the hind limbs, as readout parameter. Based on previous studies, we consider an increase of 13% (standard deviation of 10%) in weight distribution on the affected limb in time in the therapy groups as relevant in our study [67]. Sample size was calculated with a statistical power of 80% and significance level of 0.05, which led to N=8. For statistical analysis, the linear mixed model with Bonferroni's multiple comparisons test was performed.

Supplementary methods

Description of further procedures can be found in supplementary methods.

Authors contribution

MNFB designed the *in silico*, *in vitro* and *in vivo* studies, performed experiments, analyzed and interpreted the data and wrote the manuscript. RL designed the *in silico* study, analyzed and interpreted the data and wrote the manuscript. AC analyzed *in vivo* data and edited the manuscript. FTB performed *in vitro* experiments, analyzed the data and edited the manuscript. NF performed *in vivo* experiments, analyzed the data and edited the manuscript. NK performed *in vitro* and *in vivo* experiments, analyzed the data, and edited the manuscript. AAP and MGC designed the *in vivo* study, interpreted the data and edited the manuscript. YMBJ designed the *in vitro* and *in vivo* studies, interpreted the data and edited

the manuscript. LG and RN interpreted the data and edited the manuscript. GJVMvO designed the *in vitro* and *in vivo* studies, analyzed *in vivo* data, interpreted the data and edited the manuscript. All authors approved the final version of the manuscript.

Ethical statement

Animal experiments were approved by the medical ethical committee of the Erasmus MC, University Medical Center, Rotterdam, protocol number EMC 16-691-06. Human articular cartilage was obtained with the approval of Erasmus MC, protocol number MEC-2004-322 and mesenchymal stromal cells, MEC-2014-16. Written consent was not required in accordance with institutional guidelines for the use of waste surgical material, and an opt-out option was available.

Funding

This study was financially supported by the European Union's Horizon 2020 Research and Innovation Programme under the Marie Skłodowska-Curie grant agreement no. 721432 CarBon and the Reumafonds ReumaNederland (grant no. 18-1-202).

Raw data are available upon request from the corresponding author.

Conflict of interest

M.N. Ferrao Blanco, R. Lesage, N. Kops, N. Fahy, F.T. Bekedem, A. Chavli, Y.M. Bastiaansen-Jenniskens, L. Geris, M.G. Chambers, A.A. Pitsillides, R. Narcisi, G.J.V.M. van Osch. have no conflicts of interest to declare

M.G. Chambers is an employee of Eli Lilly but they did not fund this research

Acknowledgements

We would like to thank dr. Eric Farrell and Janneke Witte-Bouma for providing the MSCs. Also, the authors of the three microarrays used on this study, Daniele Belluoccio, John Bateman and Camilla Karlsson. This work was performed within the framework of the Erasmus Postgraduate School, the Medical Delta RegMed4D program and the European Union's Horizon 2020 Research and Innovation Programme under the Marie Skłodowska-Curie grant agreement no. 721432 CarBon

References

1. Cross, M., et al., *The global burden of hip and knee osteoarthritis: estimates from the global burden of disease 2010 study.* Ann Rheum Dis, 2014. **73**(7): p. 1323-30.
2. Bacon, K., et al., *Does cartilage loss cause pain in osteoarthritis and if so, how much?* Ann Rheum Dis, 2020. **79**(8): p. 1105-1110.
3. Loeser, R.F., et al., *Osteoarthritis: a disease of the joint as an organ.* Arthritis Rheum, 2012. **64**(6): p. 1697-707.

4. van der Kraan, P.M. and W.B. van den Berg, *Chondrocyte hypertrophy and osteoarthritis: role in initiation and progression of cartilage degeneration?* Osteoarthritis Cartilage, 2012. **20**(3): p. 223-32.
5. Roelofs, A.J., et al., *Identification of the skeletal progenitor cells forming osteophytes in osteoarthritis.* Ann Rheum Dis, 2020. **79**(12): p. 1625-1634.
6. Smith, M.D., et al., *Synovial membrane inflammation and cytokine production in patients with early osteoarthritis.* J Rheumatol, 1997. **24**(2): p. 365-71.
7. Benito, M.J., et al., *Synovial tissue inflammation in early and late osteoarthritis.* Ann Rheum Dis, 2005. **64**(9): p. 1263-7.
8. Saito, T., et al., *Transcriptional regulation of endochondral ossification by HIF-2alpha during skeletal growth and osteoarthritis development.* Nat Med, 2010. **16**(6): p. 678-86.
9. Ferrao Blanco, M.N., et al., *Effect of Inflammatory Signaling on Human Articular Chondrocyte Hypertrophy: Potential Involvement of Tissue Repair Macrophages.* Cartilage, 2021. **13**(2_suppl): p. 168S-174S.
10. Belluoccio, D., et al., *Sorting of growth plate chondrocytes allows the isolation and characterization of cells of a defined differentiation status.* J Bone Miner Res, 2010. **25**(6): p. 1267-81.
11. Bateman, J.F., et al., *Transcriptomics of wild-type mice and mice lacking ADAMTS-5 activity identifies genes involved in osteoarthritis initiation and cartilage destruction.* Arthritis Rheum, 2013. **65**(6): p. 1547-60.
12. Ashburner, M., et al., *Gene ontology: tool for the unification of biology. The Gene Ontology Consortium.* Nat Genet, 2000. **25**(1): p. 25-9.
13. Karlsson, C., et al., *Genome-wide expression profiling reveals new candidate genes associated with osteoarthritis.* Osteoarthritis Cartilage, 2010. **18**(4): p. 581-92.
14. Varela-Eirin, M., et al., *Targeting of chondrocyte plasticity via connexin43 modulation attenuates cellular senescence and fosters a pro-regenerative environment in osteoarthritis.* Cell Death Dis, 2018. **9**(12): p. 1166.
15. Lesage, R., et al., *An integrated in silico-in vitro approach for identification of therapeutic drug targets for osteoarthritis.* bioRxiv, 2021: p. 2021.09.27.461207.
16. Peng, Q., et al., *EPH receptor A2 governs a feedback loop that activates Wnt/beta-catenin signaling in gastric cancer.* Cell Death Dis, 2018. **9**(12): p. 1146.
17. Li, J.Y., et al., *S897 phosphorylation of EphA2 is indispensable for EphA2-dependent nasopharyngeal carcinoma cell invasion, metastasis and stem properties.* Cancer Lett, 2019. **444**: p. 162-174.
18. Irie, N., et al., *Bidirectional signaling through ephrinA2-EphA2 enhances osteoclastogenesis and suppresses osteoblastogenesis.* J Biol Chem, 2009. **284**(21): p. 14637-44.
19. Miao, H., et al., *EphA2 mediates ligand-dependent inhibition and ligand-independent promotion of cell migration and invasion via a reciprocal regulatory loop with Akt.* Cancer Cell, 2009. **16**(1): p. 9-20.
20. Pratt, R.L. and M.S. Kinch, *Activation of the EphA2 tyrosine kinase stimulates the MAP/ERK kinase signaling cascade.* Oncogene, 2002. **21**(50): p. 7690-9.
21. Pandey, A., et al., *Activation of the Eck receptor protein tyrosine kinase stimulates phosphatidylinositol 3-kinase activity.* J Biol Chem, 1994. **269**(48): p. 30154-7.

22. Kim, H.S., et al., *Role of EphA2-PI3K signaling in vasculogenic mimicry induced by cancer-associated fibroblasts in gastric cancer cells.* Oncol Lett, 2019. **18**(3): p. 3031-3038.
23. Macrae, M., et al., *A conditional feedback loop regulates Ras activity through EphA2.* Cancer Cell, 2005. **8**(2): p. 111-8.
24. Dreier, R., *Hypertrophic differentiation of chondrocytes in osteoarthritis: the developmental aspect of degenerative joint disorders.* Arthritis Res Ther, 2010. **12**(5): p. 216.
25. Choi, Y., et al., *Discovery and structural analysis of Eph receptor tyrosine kinase inhibitors.* Bioorg Med Chem Lett, 2009. **19**(15): p. 4467-70.
26. Moccia, M., et al., *Identification of Novel Small Molecule Inhibitors of Oncogenic RET Kinase.* PLoS One, 2015. **10**(6): p. e0128364.
27. Libermann, T.A. and D. Baltimore, *Activation of interleukin-6 gene expression through the NF-kappa B transcription factor.* Mol Cell Biol, 1990. **10**(5): p. 2327-34.
28. Mueller, M.B. and R.S. Tuan, *Functional characterization of hypertrophy in chondrogenesis of human mesenchymal stem cells.* Arthritis Rheum, 2008. **58**(5): p. 1377-88.
29. Farrell, E., et al., *Chondrogenic priming of human bone marrow stromal cells: a better route to bone repair?* Tissue Eng Part C Methods, 2009. **15**(2): p. 285-95.
30. Scotti, C., et al., *Recapitulation of endochondral bone formation using human adult mesenchymal stem cells as a paradigm for developmental engineering.* Proc Natl Acad Sci U S A, 2010. **107**(16): p. 7251-6.
31. Hellingman, C.A., et al., *Fibroblast growth factor receptors in in vitro and in vivo chondrogenesis: relating tissue engineering using adult mesenchymal stem cells to embryonic development.* Tissue Eng Part A, 2010. **16**(2): p. 545-56.
32. Narcisi, R., et al., *Long-term expansion, enhanced chondrogenic potential, and suppression of endochondral ossification of adult human MSCs via WNT signaling modulation.* Stem Cell Reports, 2015. **4**(3): p. 459-72.
33. van der Kraan, P.M., et al., *Development of osteoarthritic lesions in mice by "metabolic" and "mechanical" alterations in the knee joints.* Am J Pathol, 1989. **135**(6): p. 1001-14.
34. Zhang, H., D. Cai, and X. Bai, *Macrophages regulate the progression of osteoarthritis.* Osteoarthritis Cartilage, 2020. **28**(5): p. 555-561.
35. Ferrao Blanco, M.N., et al., *Intra-articular injection of triamcinolone acetonide sustains macrophage levels and aggravates osteophytosis during degenerative joint disease in mice.* Br J Pharmacol, 2021.
36. Sunderkotter, C., et al., *Subpopulations of mouse blood monocytes differ in maturation stage and inflammatory response.* J Immunol, 2004. **172**(7): p. 4410-7.
37. Geissmann, F., S. Jung, and D.R. Littman, *Blood monocytes consist of two principal subsets with distinct migratory properties.* Immunity, 2003. **19**(1): p. 71-82.
38. Scanzello, C.R. and S.R. Goldring, *The role of synovitis in osteoarthritis pathogenesis.* Bone, 2012. **51**(2): p. 249-57.
39. Miller, R.E., R.J. Miller, and A.M. Malfait, *Osteoarthritis joint pain: the cytokine connection.* Cytokine, 2014. **70**(2): p. 185-93.
40. Amato, K.R., et al., *EPHA2 Blockade Overcomes Acquired Resistance to EGFR Kinase Inhibitors in Lung Cancer.* Cancer Res, 2016. **76**(2): p. 305-18.

41. Amato, K.R., et al., *Genetic and pharmacologic inhibition of EPHA2 promotes apoptosis in NSCLC.* J Clin Invest, 2014. **124**(5): p. 2037-49.
42. Martini, G., et al., *EPHA2 Is a Predictive Biomarker of Resistance and a Potential Therapeutic Target for Improving Antiepidermal Growth Factor Receptor Therapy in Colorectal Cancer.* Mol Cancer Ther, 2019. **18**(4): p. 845-855.
43. Xiang, Y.P., et al., *Y772 phosphorylation of EphA2 is responsible for EphA2-dependent NPC nasopharyngeal carcinoma growth by Shp2/Erk-1/2 signaling pathway.* Cell Death Dis, 2020. **11**(8): p. 709.
44. Zeng, L., et al., *A Novel EphA2 Inhibitor Exerts Beneficial Effects in PI-IBS in Vivo and in Vitro Models via Nrf2 and NF-kappaB Signaling Pathways.* Front Pharmacol, 2018. **9**: p. 272.
45. Yan, D., et al., *Fibroblast growth factor receptor 1 is principally responsible for fibroblast growth factor 2-induced catabolic activities in human articular chondrocytes.* Arthritis Res Ther, 2011. **13**(4): p. R130.
46. Li, K., et al., *Tyrosine kinase Fyn promotes osteoarthritis by activating the beta-catenin pathway.* Ann Rheum Dis, 2018. **77**(6): p. 935-943.
47. Zhang, X., R. Crawford, and Y. Xiao, *Inhibition of vascular endothelial growth factor with shRNA in chondrocytes ameliorates osteoarthritis.* J Mol Med (Berl), 2016. **94**(7): p. 787-98.
48. Ferrao Blanco, M.N., et al., *Tyrosine kinases regulate chondrocyte hypertrophy: promising drug targets for Osteoarthritis.* Osteoarthritis Cartilage, 2021. **29**(10): p. 1389-1398.
49. Guo, X., et al., *The Wnt/beta-catenin pathway interacts differentially with PTHrP signaling to control chondrocyte hypertrophy and final maturation.* PLoS One, 2009. **4**(6): p. e6067.
50. Prasadam, I., et al., *ERK-1/2 and p38 in the regulation of hypertrophic changes of normal articular cartilage chondrocytes induced by osteoarthritic subchondral osteoblasts.* Arthritis Rheum, 2010. **62**(5): p. 1349-60.
51. Tang, Q., et al., *Wogonoside inhibits IL-1beta induced catabolism and hypertrophy in mouse chondrocyte and ameliorates murine osteoarthritis.* Oncotarget, 2017. **8**(37): p. 61440-61456.
52. Hunter, D.J., *Pharmacologic therapy for osteoarthritis--the era of disease modification.* Nat Rev Rheumatol, 2011. **7**(1): p. 13-22.
53. Yahara, Y., et al., *Pterosin B prevents chondrocyte hypertrophy and osteoarthritis in mice by inhibiting Sik3.* Nat Commun, 2016. **7**: p. 10959.
54. Carlson, E.L., et al., *Paroxetine-mediated GRK2 inhibition is a disease-modifying treatment for osteoarthritis.* Sci Transl Med, 2021. **13**(580).
55. Roemer, F.W., et al., *The role of radiography and MRI for eligibility assessment in DMOAD trials of knee OA.* Nat Rev Rheumatol, 2018. **14**(6): p. 372-380.
56. Sellam, J. and F. Berenbaum, *The role of synovitis in pathophysiology and clinical symptoms of osteoarthritis.* Nat Rev Rheumatol, 2010. **6**(11): p. 625-35.
57. Hong, H.N., et al., *Cancer-associated fibroblasts promote gastric tumorigenesis through EphA2 activation in a ligand-independent manner.* J Cancer Res Clin Oncol, 2018. **144**(9): p. 1649-1663.
58. Mukai, M., et al., *EphA receptors and ephrin-A ligands are upregulated by monocytic differentiation/maturation and promote cell adhesion and protrusion formation in HL60 monocytes.* BMC Cell Biol, 2017. **18**(1): p. 28.

59. Finney, A.C., et al., *EphA2 Expression Regulates Inflammation and Fibroproliferative Remodeling in Atherosclerosis.* Circulation, 2017. **136**(6): p. 566-582.
60. Huskisson, E.C., et al., *Another look at osteoarthritis.* Ann Rheum Dis, 1979. **38**(5): p. 423-8.
61. Kellgren, J.H. and R. Moore, *Generalized osteoarthritis and Heberden's nodes.* Br Med J, 1952. **1**(4751): p. 181-7.
62. Jackson, T.L., et al., *Oral Tyrosine Kinase Inhibitor for Neovascular Age-Related Macular Degeneration: A Phase 1 Dose-Escalation Study.* JAMA Ophthalmol, 2017. **135**(7): p. 761-767.
63. Richeldi, L., et al., *Efficacy and safety of nintedanib in idiopathic pulmonary fibrosis.* N Engl J Med, 2014. **370**(22): p. 2071-82.
64. Yazici, Y., et al., *A Phase 2b randomized trial of lorecivivint, a novel intra-articular CLK2/DYRK1A inhibitor and Wnt pathway modulator for knee osteoarthritis.* Osteoarthritis Cartilage, 2021. **29**(5): p. 654-666.
65. Yaeger, P.C., et al., *Synergistic action of transforming growth factor-beta and insulin-like growth factor-I induces expression of type II collagen and aggrecan genes in adult human articular chondrocytes.* Exp Cell Res, 1997. **237**(2): p. 318-25.
66. Mandl, E.W., et al., *Multiplication of human chondrocytes with low seeding densities accelerates cell yield without losing redifferentiation capacity.* Tissue Eng, 2004. **10**(1-2): p. 109-18.
67. Yuan, X.C., et al., *Electroacupuncture potentiates peripheral CB2 receptor-inhibited chronic pain in a mouse model of knee osteoarthritis.* J Pain Res, 2018. **11**: p. 2797-2808.